JOURNAL OF Applied Polymer SCIENCE

Structural, Mechanical, and Biocompatibility Analyses of a Novel Dental Restorative Nanocomposite

A. S. Khan,[1,2] F. S. L. Wong,[3] I. J. McKay,[4] R. A. Whiley,[4] I. U. Rehman[5]

[1]Interdisciplinary Research Centre in Biomedical Materials, COMSATS Institute of Information Technology, Lahore, Pakistan
[2]School of Engineering and Materials Science, Queen Mary University of London, London, United Kingdom
[3]Paediatric Dentistry, Centre for Oral Growth and Development, Barts and the London School of Medicine and Dentistry, Queen Mary University of London, London, United Kingdom
[4]Clinical and Diagnostic Oral Sciences, Barts and the London School of Medicine and Dentistry, Queen Mary University of London, London, United Kingdom
[5]Department of Material Science and Engineering, The Kroto Research Institute, University of Sheffield, Broad Lane, Sheffield S3 7HQ, United Kingdom

Correspondence to: I. U. Rehman (E-mail: i.u.rehman@sheffield.ac.uk)

ABSTRACT: Structure and biocompatibility are key parameters that determine the usefulness of dental materials for clinical use. Novel polyurethane (PU) nanocomposite material was prepared by chemically binding nanohydroxyapatite (nHA) to the diisocyanate component of the PU backbone by solvent-polymerization. nHA was incorporated into PU by the stepwise addition of monomeric units of the PU. The PU/nHA composite was analyzed by ^{13}C Nuclear magnetic resonance (structural) and X-ray diffraction (phase analysis). The tensile strength and elastic modulus was evaluated for mechanical properties. These analyses revealed linkage between the hard- and soft-segments are urethane linkage and showed high mechanical properties with increase in content of nHA. To assess biocompatibility osteoblast cells were seeded on to the material and allowed to adhere and proliferate. Osteoblast-like cell growth and proliferation was assessed by MTS assay. It was found that cells adhered and proliferated on these novel substrates. To test bacterial adhesion discs of composite with and without nHA were incubated with standardized suspensions of oral bacterium *Streptococcus sanguinis* strain NCTC 7863. PU composites with nHA exhibited biocompatibility with respect to mammalian cell growth and showed significantly reduced bacterial adhesion as compared to PU alone. © 2012 Wiley Periodicals, Inc. J. Appl. Polym. Sci. 000: 000–000, 2012

KEYWORDS: polyurethane; nanohydroxyapatite; structural analysis; mechanical properties; biocompatibility

Received 11 January 2012; accepted 14 March 2012; published online
DOI: 10.1002/app.37841

INTRODUCTION

It is desirable for dental materials to have bioactive and biocompatible properties at the interface between the material and tissue to prevent micro-leakage and ingress of bacteria. The interfacial adhesion of restorative material to dentin is important for maintaining integrity of the seal in root canal filling in both static and dynamic conditions. Improvements in adhesive technology have fostered attempts to incorporate adhesive dentistry in endodontics by introducing obturation system with a specific focus on obtaining a single cohesive unit.[1] The term "monoblock" has become familiar in the endodontic literature; however, it has generated controversial discussions among academicians and clinicians as to whether they are able to improve the quality of seal in root fillings and to strengthen roots. Monoblocks created in the root canal spaces may be classified as primary (mineral trioxide aggregate MTA), secondary (Gutta-percha and Resilon) and tertiary (EndoRez), depending on the number of interfaces present between bonding substrate and the bulk material core. MTA does not confer any perceivable benefit in root strengthening, apart from its ability to stimulate cementogenesis in apexification and root end fillings.[2] The bonding of Resilon to methacrylate resin-based sealers and root dentin is weak. Resilon as a fully polymerized material that lacks a free radical-containing oxygen inhibition layer, its bond-ability to resin based sealers has further been questioned.[3] Research studies indicated that there is no difference between Resilon and Gutta-percha in strengthening and reinforcement of roots[4,5] that challenges the concept of strengthening root-filled teeth with the new endodontic material.

Ideal obturating materials should be nonirritating to the periapical tissues and have acceptable adaptation to root canal walls. However, present filling materials have a tissue-irritating potential and techniques fail in achieving the requirement of providing a suitable linkage with tooth structure.[6] Various studies have shown that the weak link between Gutta-percha/AH Plus, Resilon/Epiphany, and dentin interfere with the goal of creating a monoblock between the root and the filling.[7]

Polyurethane (PU) and nanohydroxyapatite (nHA) have been used in a variety of biomedical applications. The interfacial linkage between PU and nHA is one of the major factors that determine the ultimate properties of the composite. The formation of apatite at the interface or bonding to already present apatite could create a much closer to natural state of restoration than present composite systems.[8,9] Very limited studies have been performed for the application of polymer/HA composites for dental restorations. These studies reported physical, thermal, mechanical,[10–12] water absorption,[13] and *in-vitro* bioactivity[14] properties of the composites. However, PU/nHA composite has not been used in dental applications. The concept of creating mechanically/chemically homogenous units "ideal monoblocks" with root dentin is challenging. Our previous studies, confirmed the biostability of newly developed nanocomposite,[15] the results of thermal properties, *in vitro* bioactivity, adhesion with root dentin were presented in subsequent studies.[16,17] The incorporation of nHA in these composites enhanced the bioactive properties, thermal stability, and increased the resistance toward hydrolytical degradation. The presence of apatite layer was observed on the surface of these samples, consequently apatite layer showed its tendency to bond with tooth structure. The presence of calcium phosphate component in composite enhanced the adhesion compared with Gutta-percha. In view of its dental application, further characterization is required including the structural, mechanical, and biological properties of the composite. It is hypothesized that a chemical coupling between PU and nHA will show better mechanical strength and demonstrates low cytotoxicity and microbial adherence.

EXPERIMENTAL

Synthesis of Hydroxyapatite

Nanohydroxyapatite (nHA) was synthesized by ammonium hydrogen phosphate 98% [$(NH_4)_2HPO_4$] and calcium nitrate tetrahydrate 99% [$Ca(NO_3)_2$. $4H_2O$] as phosphate and calcium precursors; distilled water and ethanol were used as solvent for precursors, respectively. Ammonium hydroxide was used to control the pH value. The pH value was maintained at 11. All materials were purchased from Sigma Aldrich, UK and were analytical grade. Sol-gel technique[18] was used to synthesize the nanopowder and the resulting powder was heat treated at 700°C and ground with ball milling.

Synthesis of PU-Based Composites

All chemicals used in this study were of analytical grade and purchased from Sigma Aldrich, UK. Poly (tetramethylene glycol) (PTMG : M_w 1400 g mol^{-1}) soft segment were freeze dried for 22 h prior to employing in the synthesis process. 4, 4′-methylene diphenyl diisocyanate (MDI) hard segment and 1,4-Butanediol (BDO) chain extender were used as received. *N, N*′-dimethyl formamide (DMF) were dried by 4 Å molecular sieves for 72 h and used as solvent. PU and PU/nHA composite were synthesized by a step growth polymerization method without using a catalyst as it was described in our previous study.[18] The concentration of nHA was 5, 10, 15, and 20% (wt/wt) with respect to PTMG. The *in situ* polymerization was conducted with drop wise addition of MDI and BDO in PTMG solution at 60°C. The nHA particles were added during the mixing procedure. The reaction was carried out at 80°C for 1 h and then at 110°C for further 4 h. DMF was added occasionally to the reactor when the viscosity of the reactants was too high prior to polymerization. After 4 h the experiment was finished and the solution was precipitated in ice water followed by reprecipitation in methanol to remove any unreacted MDI and low-molecular-weight polymer. The resulting composite was dried under vacuum at room temperature for 48 h. Batches of composite films (1 mm thick) were prepared by a cast solvent technique and cut into 12 mm diameter discs.

Characterizations

^{13}C-Nuclear Magnetic Resonance. ^{13}C Nuclear Magnetic Resonance (^{13}C NMR) was used to analyze the chemical composition of the composite. Five samples of each PU and PU/nHA20 were completely dissolved in tetrahydrofuran (THF) solvent and ^{13}C NMR spectra were recorded on a Bruker 600 MHz NMR spectrometer using a magnetic field frequency of 100 MHz for ^{13}C nuclei.

Scanning Electron Microscopy. The morphology and surface analysis of nHA powder and PU/nHA composite were characterized by scanning electron microscopy, SEM (JEOL 6300 JSM and Inspect FEI, The Netherlands) and energy dispersive spectroscopy (EDS) at an activation voltage of 15 kV. The samples were mounted and were sputter coated under vacuum with carbon.

X-Ray Diffraction. The X-ray powder diffraction data was collected for PU and PU/nHA composite samples using a Simens D 5000 diffractometer [Cu-Kα radiation (kα1 = 0.15406 nm)]. An attachment was used across the 2θ range. The samples were set at 1° and fixed, and the detector was scanned between 10° and 70°. A step size of 0.02° was used, with a step time of 2.5 s. Peak positions were evaluated by using software EVA^{TM} (Bruker-AXS, Germany).

Mechanical Properties. A tensile strength test was performed using an Instron (6025, Instron, MA) equipped with a 10 N load cell at room temperature. Dog-bone shape specimens were cut from cast films using an ASTM D638 standard punch and testing conditions were selected according to ASTM: D412-98a. The thickness of the films was 1 mm. Specimens were kept in a desiccator at 37°C for 24 h before testing. The specimens were stretched until break at a crosshead rate of 0.5 mm/min. Stress–strain curves were calculated, using the initial crosssectional area of the gauge section and the initial 4 mm gauge length. Elastic modulus, *E*, was obtained by calculating the slope of the initial linear region of the stress–strain curve. Ultimate tensile strength (the maximum stress achieved prior to rupture) were also obtained from the stress–strain curves. Six samples were

tested for each composite material and the mean values were statistically analyzed by using ANOVA.

Biocompatibility Analysis

Cell Proliferation. Primary rat calvarial osteoblasts isolated by explant culture and were cultured and maintained in minimal essential medium (MEM) Alpha medium (Invitrogen, UK) supplemented with 10% fetal calf serum (FCS) (Sigma Aldrich, UK), 0.3 μg/mL fungizone (Invitrogen, UK) and 50 μg/mL penicillin-50 μg/mL streptomycin (Invitrogen, UK). The cells were grown in a humidified incubator at 37°C with 5% CO_2. The MTS assay was used to determine the number of viable cells on the films. Stock solutions of MTS (2 mg/mL) (Promega, UK) in phosphate buffered saline (PBS) and 90% phenazine methosulfate (PMS) (0.92 mg/mL) (Sigma, UK) in PBS were prepared. Before use stock solutions MTS and PMS were mixed at a 20 :1 ratio to make working solution. When 90% confluence was reached cells were detached by trypsinization and the cell density adjusted to 3×10^4 cells/mL. To evaluate proliferation cells were seeded onto PU and PU/nHA20 composite films. Wells without films were used as controls. The films with cells were placed in a humidified incubator. To measure cell proliferation films transferred at days 3, 5, and 7 to a fresh 24-well plate. Films were covered with media (1 mL/well) and 200 μL of the MTS working solution added per well. The plates were incubated for 3 h and then three samples of 100 μL each were taken out from each of the wells and transferred to 96 well plates. The colorimetric measurement was then performed using a spectrophotometer at 490 nm (FLUOstar Optima, BMG Labtech). Triplicate discs of material were tested and the experiment was repeated three times. Independent student's *t*-test was performed to find out the statistical analysis and the significant difference value was $P \leq 0.05$.

Bacterial Adhesion. Oral bacterium *Streptococcus sanguinis* strain NCTC 7863 was used in this study. The cultures were incubated at 37°C in an anaerobic atmosphere (80% N_2, 10% H_2, 10% CO_2). Colonies grown overnight on Blood agar No. 2 (Oxoid, Hampshire, UK) were inoculated into 18 mL Brain Heart Infusion broth (BHI) (Oxoid, Hampshire, UK), cultured for 18 h and then harvested by centrifugation at 3,000 rpm for 10 mins at 4°C. The resulting cell pellet was washed once in 15 mL PBS and resuspended in PBS to an OD at 600 nm of 0.2 (equivalent to 5×10^8 colony forming units [cfu]/mL). Twenty-five microliter of this suspension was placed onto a disc of the material to be tested and incubated for 2 h at 37°C aerobically. After incubation any excess bacterial suspension was removed and the discs were removed into 3 mL ice cold PBS and washed 2× to remove any nonadherent bacteria. Discs were then placed in a glass universal bottle containing 12 sterile 3.5–4 mm diameter glass beads in 2 mL PBS and vortexed for 1 min to remove adherent bacteria for counting. The resulting bacterial suspension was serially diluted (10-fold). Forty microliter of each dilution was plated onto Blood agar No. 2 plates and incubated for 2 days. Colonies were counted, cfu/mL of the final (adherent) bacterial suspension determined and cfu/mm^2 disc surface were calculated. Triplicate discs of material were tested and the experiment was repeated three times. Independent student's *t*-test was performed to find out the statistical analysis and the significant difference value was $P \leq 0.05$.

RESULTS AND DISCUSSION

The comparative ^{13}C NMR pattern of PU and PU/nHA20 are given in Figure 1 and peaks tabulated in Table I. The shifting and emergence of peaks observed at 65.15–62.3 ppm and 41.50 ppm were expected because of reaction between carbon and isocyanate to form hydrogen bonded C═O and urethane linkage, respectively. The peak at 30.38 ppm is associated with soft-segment carbons adjacent to a urethane linkage. High resolution ^{13}C NMR spectra provide useful information for the identification of material compositions. The patterns for the monomeric and polymeric PU compounds in this study are highly characteristic. The ^{13}C NMR study was conducted using THF and it has been reported that N—H proton signals were sensitive to the environment such as solvent, water, and temperature. The chemical shift in the ^{13}C NMR spectra for PU and related materials in various solvents have been described by Kricheldorf and Hull.[19] The peaks of the ^{13}C NMR spectrum for PU [Figure 1(a)] showed peaks at various regions. The signals at 153.12, 154.39, and 138.62–139.23 ppm were due to quaternary carbon. The C═O resonance signals of the PU were assigned at 153.12 ppm. The other small peak at 154.39 ppm was assigned to urethane. The signals at 135.92–139.23 ppm were due to ipso carbons (C-1). The peak at 136 ppm range was assigned to quaternary MDI ring carbons (C12 and C15), and the peak at 119.16 and 129 ppm were assigned to protonated aromatic MDI carbons (C9/C13 and C8/C14). There were five different primary peaks that could be assigned to aromatic carbons ranging from 118.94 to 139.23 ppm. The intensities of signals at 120–121 ppm were halves of the signals at 118–119 ppm, so signals at 120–121 ppm must be due to para carbons (C4). The signals at 118–119 ppm were due to ortho carbon (C2).[20] The aromatic carbons served as characteristic signals of anomalous linkages. The C2 signals were the easiest ones to detect. They were isolated from the main urethane signals and their intensities were stronger because of attaching a proton and were duplicated by the symmetry. The signals at 71.77 to 67.02 ppm were attributed to the methyleneoxy carbon of PTMG. Figure 1(a, b) has shown comparative pattern of PU and PU/nHA20 and shifting and emergence of peaks were observed. The new peaks were observed at 65.15, 62.3, and 41.50 ppm, which were due to hydrogen bonded C═O and urethane formation, respectively after the reaction of carbon and isocyanate to form hydrogen bonded. The methyleneoxy carbon attached to —CONH showed peaks at 65.01 ppm,[21] while the peak at 64.76 ppm was assigned to those soft-segment carbons that was adjacent to oxygen. The methylene group was also seen at 25.27–28.09 ppm.[22] The peak at 30.38 ppm was associated with soft-segment carbons that were adjacent to a urethane linkage. The smaller peak at 41.23 ppm was attributed to methylene carbon in MDI hard segment. The shifting of peak was expected because of availability of more hydroxyl group and this group showed affinity toward isocyanate. The hydrogen bonded urethane-carbonyl (N—H···C═O) were found and it was observed that the peak of urethane-carbonyl hydrogen bonding was shifted with the increase in concentration of nHA. The higher concentration of nHA helped in the formation of strong covalent and hydrogen linkages. The strong bonding between organic and inorganic components of restorative materials improves the properties and

Applied Polymer SCIENCE

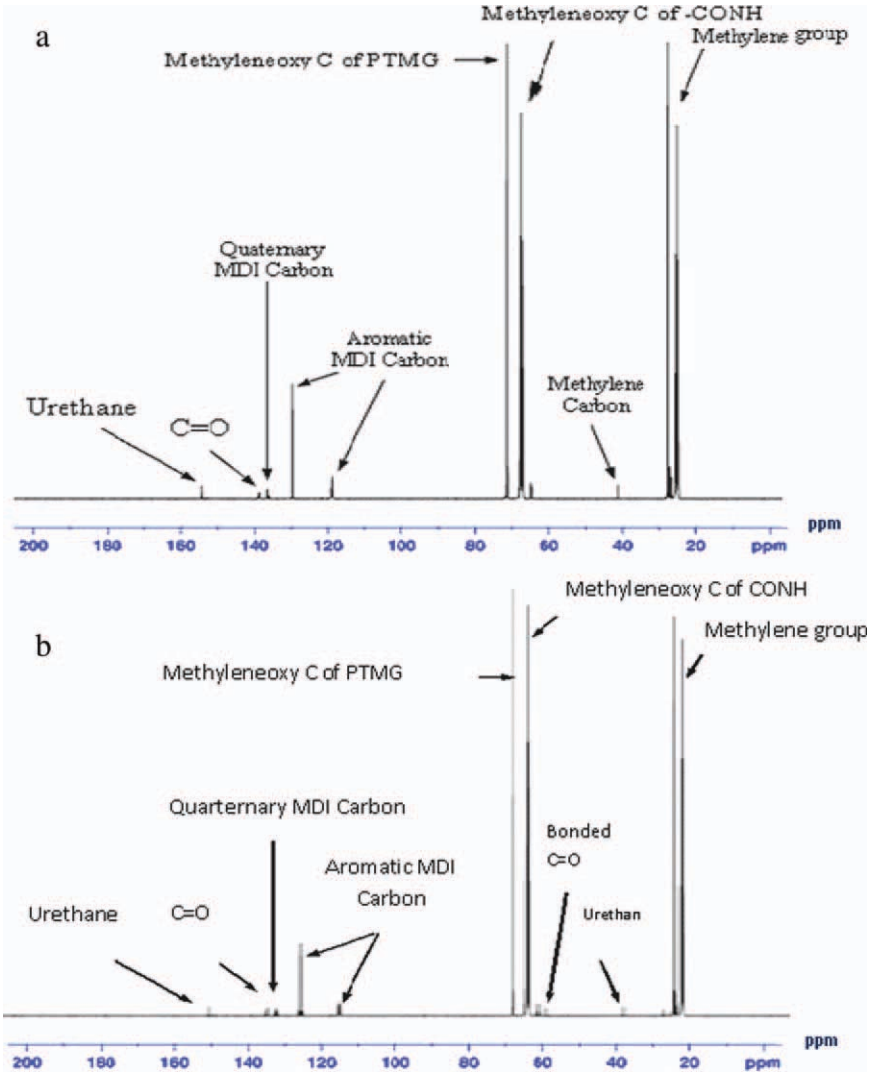

Figure 1. ^{13}C NMR peaks of (a) PU and (b) PU/nHA20 composite. [Color figure can be viewed in the online issue, which is available at wileyonlinelibrary.com.].

makes it applicable for clinical application with better results. Isocyanates are very reactive chemicals and are well known for their role in producing PUs. The structural analysis showed that the isocyanate group of MDI reacted mainly with hydroxyl (OH) group of nHA. The NCO group on benzene terminal reacted with OH group of nHA and formed the urethane linkage. The expected reaction of nHA and isocyanate are as follow:

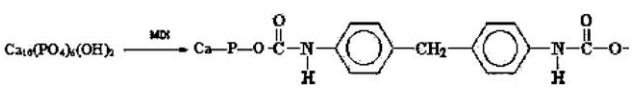

where $Ca_{10}(PO_4)_6(OH)_2$ is hydroxyapatite.

Because of the relatively complex structure of nHA, it was difficult to propose that PU could bond with apatite structure. It was expected that there was sharing of bond between —C, —O, and apatite structure. The —O and —C have charges before reaction and appeared as N=C=O, but after bonding HN—C—O showed the dipole moment. Variables such as volume fraction of inorganic fillers, particle size distribution, bonding between resin matrix, and filler particles have significant effect on properties of dental composites.

SEM images [Figure 2(a)] showed the morphological patterns of particles, which exhibited the nanostructure of hydroxyapatite particles. The observed particle sizes were in the range of 40–150 nm. To confirm the presence of nHA in polymer matrix, EDS was performed with SEM. The elements of calcium and phosphate showed their presence in PU/nHA composite [Figure 2(b)]; however, it was not dispersed separately on the surface; the nHA particles were fully embedded in the PU matrix. The structural characteristics of HA are affected by the synthetic precursors, pH values, reaction temperature, and posttreatment processes including aging and heat treatment.[23] The nHA is of biological interest because of its similarity in chemical composition and size to the mineral in teeth and bones. Thus, it may create a bioactive bond between the material and the tooth structure such as enamel and dentin, and provides better mechanical properties because of its high surface area to volume,

Table I. ^{13}C NMR Spectral Peaks Observed from PU and PU/nHA20 Composites

Peaks (ppm)	Assignments	References
154.39	Quaternary carbon of urethane	15
153.12	Quaternary carbon of urethane	15
139.23	Quaternary carbon of C=O	15
138.62	Quaternary carbon of MDI	15
136	MDI ring carbon	15
129	Protonated aromatic MDI carbon and/or CH	15
119.16	Protonated aromatic MDI carbon and/or $-CH_2$	15
71.77	Methyleneoxy carbon of PTMG	17
67.02	Methyleneoxy C of —CONH	16
65.15-62.3	bonded C=O	16
41.50	Urethane	16
41.23	Methylene carbon	17
28.09-25.27	Methylene group	17

superior chemical homogeneity, and micro-structural uniformity.[24] It is established that the presence of Ca^{2+} stimulates osteoblastic proliferation and depress osteoclast-mediated bone resorption through negative feedback loops[25] and high concentration of P induce osteoblasts apoptosis.[26] Higher concentration of Ca^{2+} promotes osteoblastic differentiation, leading to bone mineralization. This response contributes to maintenance of bone homeostasis, and the differential reactivity.[27]

In XRD study, PU samples showed [Figure 3(a)] a broad band, which was due to presence of small crystalline structure or diffraction form large crystal. This result suggested that the broad band at 20° was that of crystalline phase. The soft-segments formed crystalline structure in the segmented PU due to their long order structure. Rahman and Kim[28] studied the XRD pattern of different soft-segments (PTMG, PPG, PTAd, and PCL) and it was observed that all polyols have a crystalline structure, but none of them showed a sharp crystalline peak. The hard degree of crystallinity depends on the functional groups content. The XRD pattern of PU/nHA composites [Figure 3(b–e)] showed low intensity of nHA peak as compare to PU, which was due to the presence of PU on outer surface and arrangement of nanoparticles. If the dispersed atoms were not arranged periodically or regularly, but in independent manner, the rays scattered in a random phase and weak. However, if the atoms arranged periodically, then the scattering pattern should be strong because the scattered rays cancelled each other. The diffraction peak from partially ordered structure formed at hard-segment domain where interchain attractions such as dipole–dipole interaction and hydrogen bonding brought the hard-segment together. The polymeric chain was dynamic and flexible, but the presence of peak supported the presence of hard segment in PU.

Elastic modulus, ultimate tensile strength, and percent elongation at break were determined from stress–strain plots for each sample. The hard-segment content of all samples was same and all samples showed elastomeric behavior in tests. The ultimate tensile strength and elastic modulus values of PU and PU/nHA

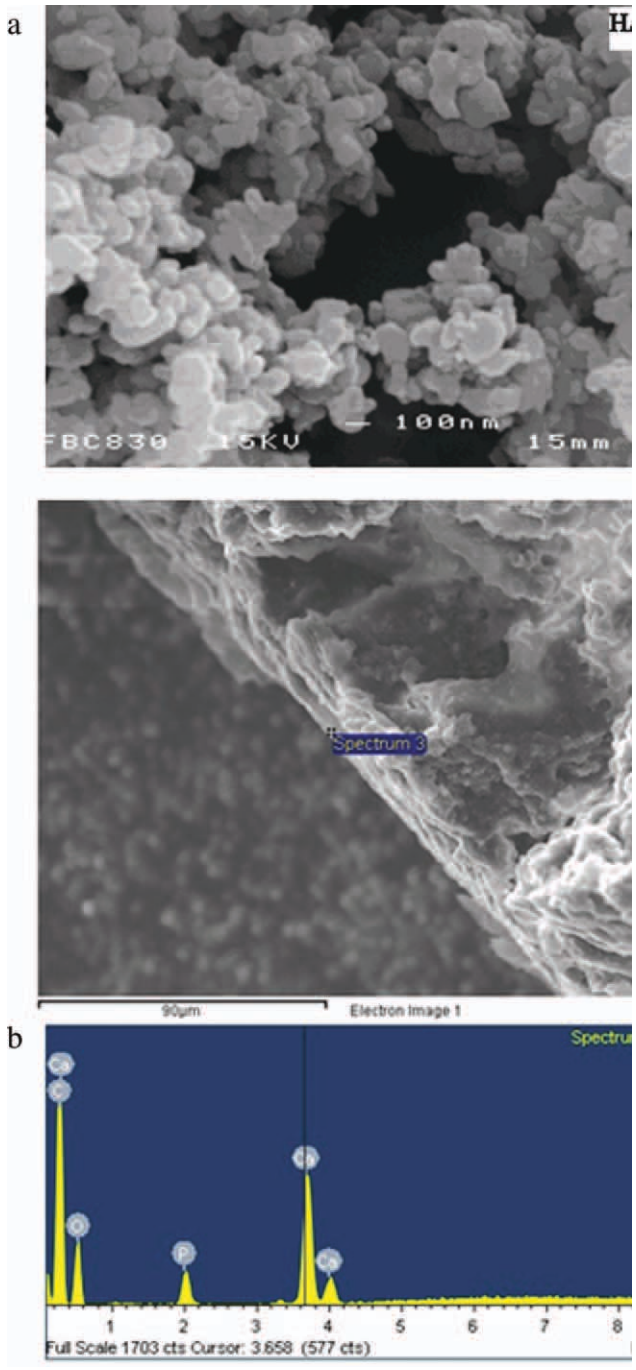

Figure 2. SEM images of (a) nHA and (b) crosssection of PU/nHA composites, EDS analysis confirms the presence of calcium phosphate contents in the composite. [Color figure can be viewed in the online issue, which is available at wileyonlinelibrary.com.].

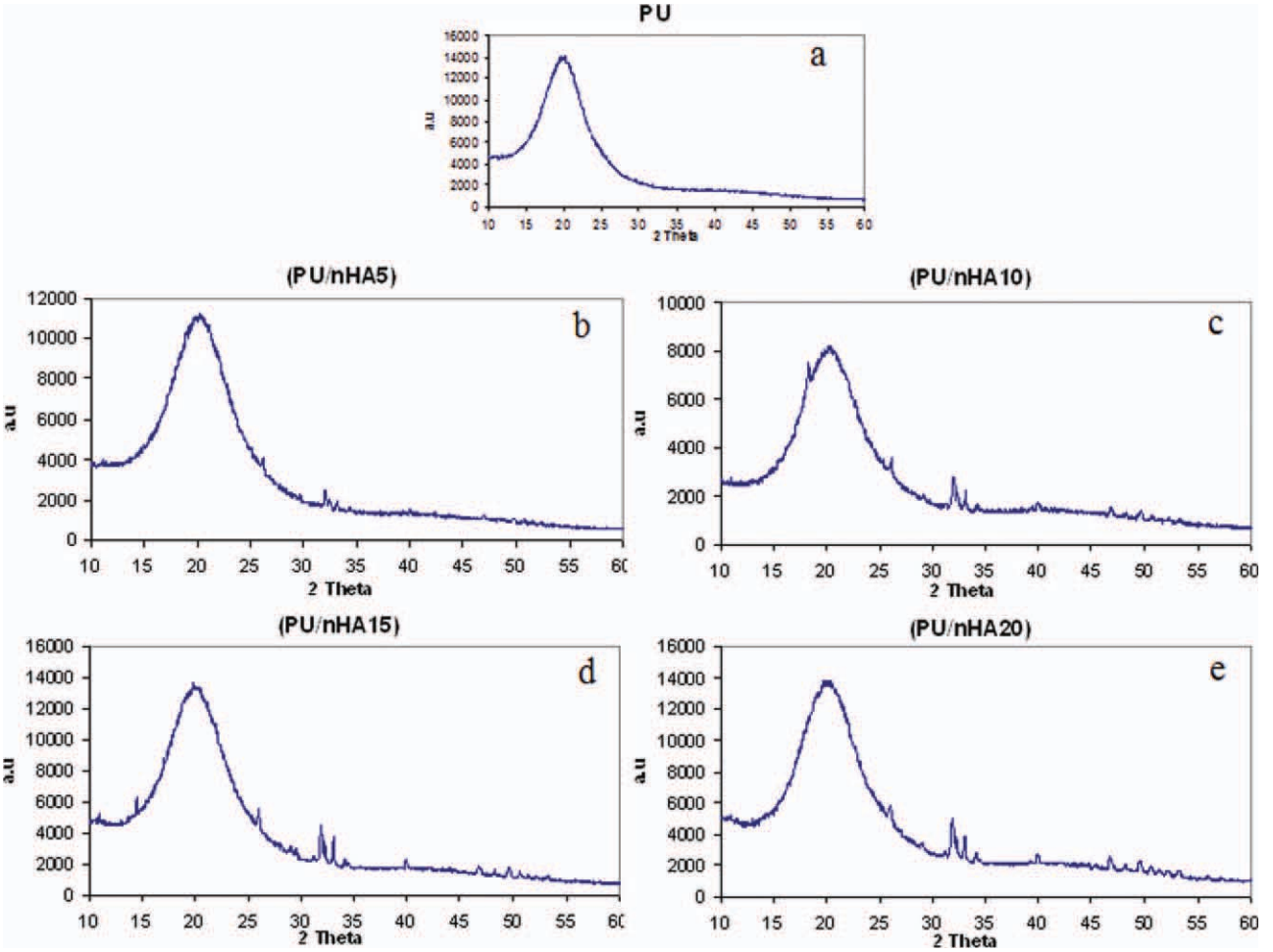

Figure 3. X-ray diffraction pattern of (a) PU, (b) PU/nHA5, (c) PU/nHA10, (d) PU/nHA15, and (e) PU/nHA20. [Color figure can be viewed in the online issue, which is available at wileyonlinelibrary.com.].

composite is given in Figure 4(a, b), respectively. The ultimate tensile strength values of PU/nHA composite (PU/nHA20–33.4 ± 3.2 MPa) increased with the increase in concentration of nHA in composite. The elastic modulus of PU/nHA20 composite (127.8 ± 27.6 MPa) was also markedly higher ($P \leq 0.05$) than that of PU (76.4 ± 10.3 MPa). Generally, all materials were elastomeric with an elongation at break of over 300%; however, it was decreased as the nHA content was increased. Sample with 5 wt % nHA content showed similarity with control PU in case of mechanical properties, which did not affect the mechanical properties of composite. However, 20 wt % nHA contents showed significant difference ($P \leq 0.05$) than PU. In comparison with existing obturating materials, this novel composite shows higher values. The reported tensile strength of Gutta-percha and Resilon is 6.0 ± 1.2 and 8.1 ± 2.3 MPa, respectively, whereas the elastic modulus of Gutta-percha and Resilon is 78.7 ± 23.4 MPa and 86.6 ± 42.2MPa, respectively.[29] These materials cannot reinforce the root because they do not adhere to the root canal wall. The elastic modulus and tensile strength of dentin are about 16 GPa and 36–100 MPa,[30] respectively. Theoretically, a material bonded to dentin should have a similar elastic modulus to that of dentin to avoid stress concentration along the interface. The higher elastic modulus of PU/nHA20 composite (127.8 MPa) should contribute a greater reinforcing effect to the roots. The tensile strength of PU/nHA composite (33.4 MPa) is also closer to that of dentin than those of Gutta-percha (6.0 MPa) and Resilon (8.1 MPa).

In vitro studies showed that neither PU nor PU/nHA20 were cytotoxic to osteoblast-like cells. Figure 5 showed cell proliferation as measured by MTS assay. Cells on film substrates continued to proliferate and remained viable cells up to 7 days. Significant difference ($P \leq 0.05$) was observed for control, PU and PU/nHA20 from day 1 to 7; however, the difference between PU and PU/nHA20 was not significant. In this study, polyetherurethane was used, which was hydrolytically resistant and showed prolonged stability. The cellular behavior, in terms of cell adhesion and growth pattern was investigated. The cells were seeded on the surface of PU, and few migrated to polystyrene surface in the plate. This movement shows that the cells were healthy. As the cells were in direct contact with the samples, it was shown that no toxic substance was released from the samples that would cause cellular damage.

The general concept of cell interaction demonstrates that cells attach much more readily to hydrophilic materials than to hydrophobic surface. The hydrophilic/hydrophobic nature of

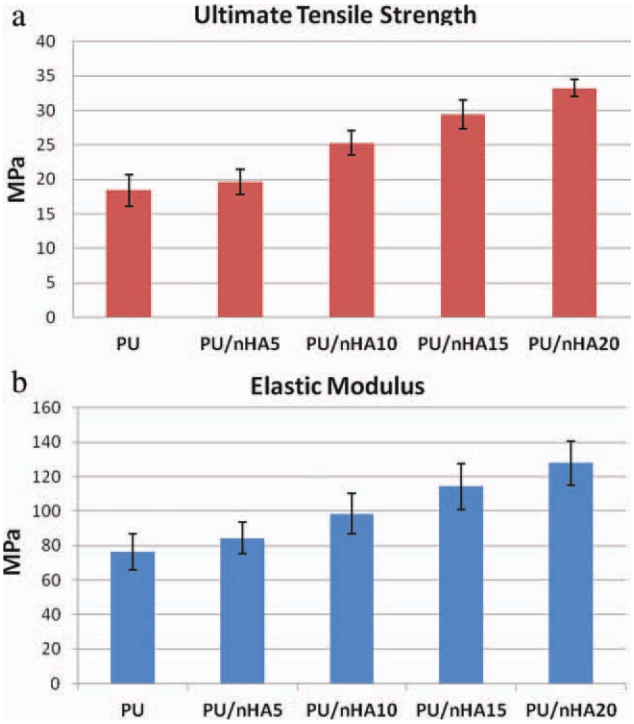

Figure 4. (a) Ultimate tensile strength and (b) elastic modulus of PU and PU/nHA composites, where significant difference ($P \leq 0.05$) was observed between PU and PU/nHA20 values. [Color figure can be viewed in the online issue, which is available at wileyonlinelibrary.com.].

this novel material was previously analyzed by contact angle measurement.[15] The degree of contact angle allows characterizing the surface wettability of a material, and can act as an indicator of its hydrophilicity/hydrophobicity. An increasing contact angle means a decrease of surface wettability, i.e., more hydrophobic. It was found by our group that surface contact angle increased with the increase in nHA content. It was shown that PU/nHA20 was more hydrophobic than PU and the result of the present study also showed that PU (comparatively less hydrophobic) had slightly higher ($P \geq 0.05$) cell proliferation and differentiation than PU/nHA20 (more hydrophobic). The

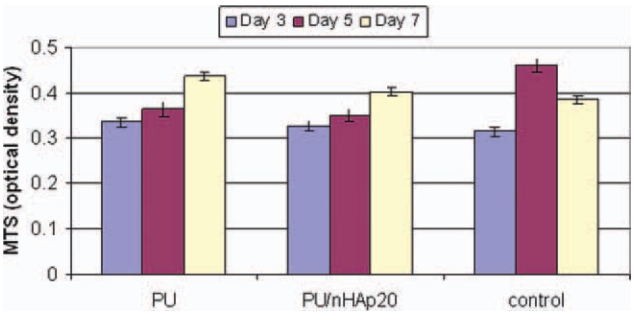

Figure 5. Cell culturing values of PU, PU/nHA20, and control group conducted in triplicate. Significant difference ($P \leq 0.05$) was observed for control, PU and PU/nHA20 from day 1 to 7; however, the difference between PU and PU/nHA20 was not significant. [Color figure can be viewed in the online issue, which is available at wileyonlinelibrary.com.].

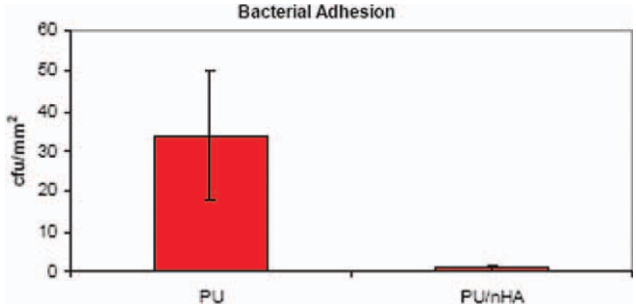

Figure 6. Bacterial adhesion values for PU and PU/nHA20. [Color figure can be viewed in the online issue, which is available at wileyonlinelibrary.com.].

authors also observed that increasing hydrophobicity led to improvement of cell adhesion and spreading. PU and PU/nHA20 are high elasticity so they could tolerate the micromechanical forces from the cells. It is expected that cells proliferated on the dispersed phase of hard-segments. The hard-segments facilitate the development of focal adhesions, thus allowing cell growth. The effect of HA properties on tissue response is not yet been fully understood. It is possible to assess the overall cell viability in the presence of HA and it has been shown that viability levels are similar across different HA concentrations.[31] The results of the present study showed that the samples with nHA exhibited attachment and proliferation of cells, which confirmed its level of biocompatibility. The nanostructures provided dense surface that increased surface energy, which should promote initial attachment and spreading of cells.[32] Cell proliferations appeared to be inversely related to the HA particle size and it is suggested that nHA particles could stimulate more osteoblastic proliferation when compared to nHA. This may be due to enhanced interfacial adhesion of nHA to cells and high surface area per HA volume for cell growth, which in turn might result in increased cellular adherence and proliferation.[33] The morphology of HA was another parameter that apparently influenced the biological activity. The cell experiments showed that nHA with spherical structure showed more favorable properties than rod-like HA for osteoblasts.[33,34] In view of this, some factors are important in determining the cell growth on PU and PU based composites i.e., surface morphology and the existence of a dispersed phase (hard/soft), hydrophilic (less hydrophobic) property, and surface energy of materials.

The cfu/mm^2 of *Streptococcus sanguinis* strain (NCTC 7863) that adhered to the materials for *in vitro* bacterial adhesion study is given in Figure 6. Significantly, more bacteria adhered to PU than PU/nHA20 composite. The mean cfu/mm^2 of adherent bacteria for PU and PU/nHA20 composite were 34 $\pm$ 16.15 and 1.0 $\pm$ 0.83 cfu/disc, respectively ($P \leq 0.05$). The *in vitro* adhesion assay carried out here was under static and submerged conditions and in a nonnutrient medium (i.e., PBS). Adhesion of bacteria to dental materials is the initial event leading to colonization, potentially resulting in infection, and caries.[35] Endodontic microorganisms have a high affinity to existing root canal filling materials, especially to Gutta-percha.[36] Another study showed no significant difference in bacterial

adhesion between Gutta-percha and Resilon.[37] The initial rate of microbial adhesion to a surface has been described as a first order dependency on concentration. The adhesion of bacteria is not related to surface hydrophobicity/hydrophilicity and it has been suggested that the number of bacteria adhering within the first hour of initial colonization is much more strain dependent than substratum dependent.[38,39] This study showed that fewer bacteria adhere to material PU/nHA20 when compared with PU. It has been reported that surface modification can achieve reduced bacterial adhesion. Clinical studies have indicated that plaque accumulated at lesser extent on ceramic material as compared to the surfaces of polymers. Surface properties such as steric hindrance, surface roughness, and surface topography all affect attachment of bacteria.[40] Clinically this novel monoblock system has potential to achieve homogeneous units with tooth structure and allow bonding to dentin. These findings suggest that irritant components of existing composite resins should be replaced by more biocompatible substances to avoid risk factors for the health of patients and dental personnel. Subsequent biofilm formation and persistence of microorganisms in root canals on these materials could be prevented.

CONCLUSIONS

^{13}C NMR spectra confirmed the urethane and carbonyl bonds and linkage between hard- and soft-segment and for PU and PU/nHA composites. This grafting could be advantageous for the coupling of osteoconductive fillers in polymer composite with PU. Covalent bonding of nHA with PU has the potential to improve the interface of nanocomposite matrix, therefore leading to significant improvement of the bioactive, bonding and mechanical properties. The biocompatibility showed that cells proliferated on the surface; whereas, more growth was observed with PU because of hydrophilic nature. In comparison there was 97.09% reduction in bacteria adhering to the grafted composite as compared to PU. This work indicates that nHA modified composites help in cell proliferation and controlling the formation of bacterial biofilm in general. Osteoblast culture has been commonly used to evaluate the material's surface characterization on biocompatibility and *Streptococcus sanguinis* is one of first bacterium to colonize tooth surfaces, by forming dental plaque, which leads to dental caries, periodontal diseases, and alteration of dental restorations. It is worth to note that in our *in vitro* study the osteoblast-like cells and *Streptococcus sanguinis* may not be able to present the real situation as occurred *in vivo*. However, we present the primary investigations, which provide insight into the biocompatibility of novel composite. Therefore, further studies need to be carried out to clarify the biocompatibility with connective tissues, fibroblasts, and other oral bacteria in order to understand the real underlying. The long-term *in vivo* studies will have to establish whether these *in vitro* results are representative for the *in vivo* behavior of biocompatibility.

ACKNOWLEDGMENTS

The authors would like to thank Dr. Greg Coumbarides (School of Biological and Chemical Sciences, Queen Mary University of London) and Ahmed Talal (School of Engineering and Materials Science, Queen Mary University of London) for their input in ^{13}C-NMR characterization and cell culturing, respectively.

REFERENCES

1. Onay, E. O.; Ungor, M.; Ari, H.; Belli, S.; Ogus, E. *Oral. Surg. Oral. Med. Oral. Pathol. Oral. Radiol. Endod.* **2009,** *107*, 879.
2. Tay, F. R.; Pashley, D. H. *J. Endod.* **2007,** *33*, 391.
3. Stuart, C. H.; Schwartz, S. A.; Beeson, T. J. *J. Endod.* **2006,** *32*, 350.
4. Gesi, A.; Raffaelli, O.; Goracci, C.; Pashley, D. H.; Tay, F. R.; Ferrari, M. J. *Endod.* **2005,** *31*, 809.
5. Hiraishi, N.; Papacchini, F.; Loushine, R. J.; Weller, R. N.; Ferrari, M.; Pashley, D. H.; Tay, F. R. *Inter. Endod. J.* **2005,** *38*, 753.
6. Enkel, B.; Dupas, C.; Armengol, V.; Adou, J. A.; Bosco, J.; Daculsi, G.; Jean, A.; Laboux, O.; LeGeros, R. Z.; Weiss, P. *Ex. Rev. Med. Dev.* **2008,** *5*, 475.
7. Kaya, B. U.; Kececi, A. D.; Orhan, H.; Belli, S. *Int. Endod. J.* **2008,** *41*, 211.
8. Mjor, I. A.; Moorhead, J. E. *Int. Dent. J.* **2000,** *50*, 361.
9. Engqvist, H.; Shultz-Walz, J. E.; Loof, J.; Botton, G. A.; Mayer, D.; Phaneuf, M. W. *Biomaterials* **2004,** *25*, 2781.
10. Chen, L.; Yu, Q.; Wang, Y.; Li, H. *Dent. Mater.* **2011,** *27*, 1187.
11. Arcis, R. W.; Lopez-Macipe, A.; Toledano, M.; Osorio, E.; Rodriguez-Clemente, R.; Murtra, J.; Fanovich, M. A.; Pascual, C. D. *Dent. Mater.* **2002,** *18*, 49.
12. Labella, R.; Braden, M.; Deb, S. *Biomaterials* **1994,** *15*, 1197.
13. Santos, C.; Clarke, R. L.; Braden, M.; Guitian, F.; Davy, K. W. *M. Biomaterials.* **2002,** *23*, 1897.
14. Deb, S.; Aiyathurai, L.; Roether, J. A.; Luklinska, Z. B. *Biomaterials.* **2005,** *26*, 3713.
15. Khan, A. S.; Aziz, M. S.; Paul, D.; Wong, F.S. L.; Rehman, I.U. J. *Bionanosci.* **2008,** *2*, 75.
16. Khan, A. S.; McKay, I. J.; Wong, F.S. L.; Rehman, I.U. *J. Dent. Res.* **2008,** *87*, (Special Issue C), 0017.
17. Khan, A. S.; Hassan, K. R.; Bukhari, S. F.; Wong, F.S. L.; Rehman, I.U. J. *Biomed. Mater. Res. B: Appl. Biomater.* **2011,** Accepted, JBMR-B-11-0124.R2.
18. Khan, A. S.; Ahmed, Z.; Edirisinghe, M. J.; Wong, F. S. *L.; Rehman, I.U. Acta. Biomater.* **2008,** *4*, 1275.
19. Kricheldrof, H. R.; Hull, W. E. *Macromol. Chem.* **1981,** *182*, 1177.
20. Kaji, A.; Arimatsu, Y.; Murano, M. J. *Polym. Sci. A: Polym. Chem.* **1992,** *30*, 287.
21. Prasath, R. A.; Nanjundan, S.; Pakula, T.; Klapper, M. *Eur. Polym. J.* **2004,** *40*, 1767.
22. Wang, Y. Z.; Hsu, Y. C.; Wu, R. R.; Kao, H. M. *Syn. Met.* **2003,** *132*, 151.
23. Lacefield, W. R. *Ann. N Y Acad. Sci.* **1998,** *523*, 72.
24. Zhu, X.; Eibl, O.; Berthold, C.; Scheideler, L.; Geis-Gerstorfer, J. *Nanotechnology* **2006,** *17*, 2711.

25. Zaidi, M.; Kerby, J.; Huang, C. L.; Alam, T.; Rathod, H.; Chambers, T. J.; Moonga, B. S. *J. Cell Phys.* **1991,** *149*, 422.
26. Meleti, Z.; Shapiro, I. M.; Adams, C. S. *Bone* **2000,** *27*, 359.
27. Maeno, S.; Niki, Y.; Matsumoto, H.; Morioka, H.; Yatabe, T.; Funayama, A.; Toyama, Y.; Taguchi, T.; Tanaka, J. *Biomaterials* **2005,** *26*, 4847.
28. Rahman, M. M.; Kim, H. D. *J. Appl. Polym. Sci.* **2007,** *104*, 3663.
29. Williams, C.; Loushine, R. J.; Weller, R. N.; Pashley, D. H.; Tay, F. R. *J. Endod.* **2006,** *32*, 553.
30. Sano, H.; Ciucchi, B.; Matthews, W. G.; Pashley, D. H. *J. Dent. Res.* **1994,** *73*, 1205.
31. Oliveira, J. M.; Rodrigues, M. T.; Silva, S. S.; Malafaya, P. B.; Gomes, M. E.; Viegas, C. A.; Dias, I. R.; Azevedo, J. T.; Mano, J. F.; Reis, R. L. *Biomaterials* **2006,** *27*, 6123.
32. Li, H.; Khor, K. A.; Chow, V.; Cheang, P. J. *Biomed. Mater. Res. A* **2007,** *82*, 296.
33. Shi, Z.; Huang, X.; Cai, Y.; Tang, R.; Yang, D. *Acta. Biomater.* **2009,** *5*, 338.
34. Zhao, Q.; Wang, C.; Liu, Y.; Wang, S. *Int. J. Adhes. Adhes.* **2007,** *27*, 85.
35. Berlot-Moirez, S.; Djavid, G. P.; Montdargent, B.; Jozefowicz, M.; Migonney, V. *ITBM-RBM* **2002,** *23*, 102.
36. Senges, C.; Wrbas, K. T.; Altenburger, M.; Follo, M.; Spitzmuller, B.; Wittmer, A.; Hellwig, E.; Al-Ahmad, A. *J. Endod.* **2011,** *37*, 1247.
37. Shin, S.-J.; Jee, S.-W.; Song, S.-W.; Song, J.-S.; Jung, I.-Y.; Cha, J.-H. J. *Endod.* **2008,** *34*, 445.
38. Gottenbos, B.; van der Mei, H. C.; Busscher, H. J. *J. Biomed. Mater. Res.* **2000,** *50*, 208.
39. Karakecilci, A. S.; Gumusderelcioaglu, M. J. *Biomater. Sci.: Polym. Ed.* **2002,** *13*, 185.
40. Vladkova, T. J. *Uni. Chem. Tech. Metallur.* **2007,** *42*, 239.